

REPORT DOCUMENTATION PAGE			<i>Form Approved</i> <i>OMB No. 0704-0188</i>		
Public reporting burden for this collection of information is estimated to average 1 hour per response, including the time for reviewing instructions, searching existing data sources, gathering and maintaining the data needed, and completing and reviewing this collection of information. Send comments regarding this burden estimate or any other aspect of this collection of information, including suggestions for reducing this burden to Department of Defense, Washington Headquarters Services, Directorate for Information Operations and Reports (0704-0188), 1215 Jefferson Davis Highway, Suite 1204, Arlington, VA 22202-4302. Respondents should be aware that notwithstanding any other provision of law, no person shall be subject to any penalty for failing to comply with a collection of information if it does not display a currently valid OMB control number. PLEASE DO NOT RETURN YOUR FORM TO THE ABOVE ADDRESS.					
1. REPORT DATE (DD-MM-YYYY) 03/15/2012		2. REPORT TYPE Final Technical		3. DATES COVERED (From - To) Dec 2008 – Sept 2011	
4. TITLE AND SUBTITLE Spin-Dependent Phenomena in Graphene			5a. CONTRACT NUMBER		
			5b. GRANT NUMBER N00014-09-1-0117		
			5c. PROGRAM ELEMENT NUMBER		
6. AUTHOR(S) Kawakami, Roland			5d. PROJECT NUMBER		
			5e. TASK NUMBER		
			5f. WORK UNIT NUMBER		
7. PERFORMING ORGANIZATION NAME(S) AND ADDRESS(ES) REGENTS OF THE UNIVERSITY OF CALIFORNIA AT RIVERSIDE 200 UNIVERSITY OFFICE BLDG RIVERSIDE, CA 92521-0123			8. PERFORMING ORGANIZATION REPORT NUMBER		
9. SPONSORING / MONITORING AGENCY NAME(S) AND ADDRESS(ES) Office of Naval Research 875 North Randolph Street Arlington, VA 22203-1995			10. SPONSOR/MONITOR'S ACRONYM(S)		
			11. SPONSOR/MONITOR'S REPORT NUMBER(S)		
12. DISTRIBUTION / AVAILABILITY STATEMENT Approved for public release; distribution is unlimited					
13. SUPPLEMENTARY NOTES none					
14. ABSTRACT Graphene is attractive for spintronics due to spin transport at room temperature with long spin diffusion lengths. During this grant period, two important aspects have been investigated: (1) Spin injection and transport in graphene, (2) Spin and charge transport in doped graphene. Main results include the first demonstration of tunneling spin injection into graphene, identification of contact effects as a major source of spin relaxation, realization of high spin injection efficiency, long spin lifetimes in bilayer graphene, the first in-situ transport study of transition metal doping of graphene including studies on graphene spin valves. These results have been at the forefront of graphene spintronics.					
15. SUBJECT TERMS graphene, spintronics, spin transport					
16. SECURITY CLASSIFICATION OF:			17. LIMITATION OF ABSTRACT UU	18. NUMBER OF PAGES 11	19a. NAME OF RESPONSIBLE PERSON Ursula Prins
a. REPORT U	b. ABSTRACT U	c. THIS PAGE U			19b. TELEPHONE NUMBER (include area code) (951)827-4808

Final Technical Report

ONR grant: N00014-09-1-0117
Spin-Dependent Phenomena in Graphene
PI: Roland Kawakami, UC Riverside
12/1/2008 – 9/30/2011

I. Overview

Graphene is an attractive material for spintronics due to its high mobility and the low intrinsic spin-orbit and hyperfine coupling, which should lead to excellent spin transport properties. In 2007, graphene became the first material to exhibit gate tunable spin transport and spin precession at room temperature [12]. However, the spin injection efficiency was low and the spin lifetime was much shorter than predicted theoretically. These issues defined the immediate challenges for the field. The original goals of this project were to investigate two broad directions in graphene spintronics: (1) Spin injection and transport in graphene: significantly improve the characteristics of spin injection and spin lifetime; explore novel geometries such as *pn* junctions and nanoribbons; investigate spin transport in epitaxial graphene. (2) Spin transport in doped graphene: investigate the effects of surface impurity scattering on charge and spin transport; find evidence for magnetism in doped graphene via exchange fields; generate spin-Hall effect generated by spin-orbit fields. We have made substantial progress in both of these areas including some breakthrough results that has established our group as among the top two groups in graphene spintronics.

(1) Spin Injection and Transport in Graphene

We have made important progress in spin injection and transport [1,2,3,7,9,10] including: Tunneling spin injection into graphene. The low spin injection efficiency into graphene is due to the conductivity mismatch between the ferromagnetic metal (Co) and the single layer graphene (SLG). To alleviate this problem and enhance the spin injection efficiency, we grew atomically smooth MgO tunnel barrier with TiO₂ seed layer. With tunneling contacts, the non-local spin signal was found to be as high as 130 Ω at room temperature, with a spin injection efficiency of 30%. This is currently the highest spin injection efficiency observed in graphene spin valves [7]. Long spin lifetimes in graphene. Enhanced spin lifetimes are observed using tunneling contacts [7]. This indicates that the short spin lifetimes reported before are due to the contact-induced spin relaxation from the ferromagnetic electrodes. Using tunneling contacts, we observed the spin lifetimes as high as 771 ps in single-layer graphene (SLG), 1.0 ns at 4 K in SLG, and 6.2 ns at 20 K in bilayer graphene (BLG) [9]. These are currently the highest values reported in the literature. At low temperatures, contrasting behaviors of gate voltage dependence of the spin lifetime are observed between SLG and BLG, which suggest different mechanisms for spin relaxation in SLG and BLG [9].

(2) Spin and Charge Transport in Doped Graphene

Due to the extreme surface sensitivity of graphene, there is a unique opportunity to modify the spin-dependent properties of graphene through a proximity effect. By introducing adatoms or thin films on top of graphene, one could induce exchange fields, tunable spin-orbit coupling, or hyperfine fields. These will be extremely useful for manipulation of spin in graphene. Our

studies utilize *in situ* transport measurements, which allow adsorbates to be deposited in ultrahigh vacuum and transport measurements to be taken without exposing the sample to air. We have several results [4,5,6,8] including:

Charged impurity scattering and charge transfer from transition metal impurities: We performed the first *in situ* study of transition metal doping on graphene. For adsorbates deposited onto graphene at low temperature to keep the adatoms separated (i.e. to avoid aggregation), we found that all materials studied including Fe, Ti, Au, and Pt donated electrons to graphene. This was especially surprising for Pt, which has a bulk workfunction of ~ 6.0 eV that is much larger than graphene (~ 4.5 eV). In such a case, one would expect the Pt to act as an electron acceptor. This shows for atomic adsorbates (or small clusters), the simple consideration of bulk workfunction is insufficient to not applicable [4]. We also investigated the role of clustering [5] and the role of insulating vs metallic character of the adsorbates [8].

Role of charged impurity scattering on spin relaxation: By investigating the effect of gold dopants on spin transport, we concluded that charged impurity scattering is not the dominant source of spin relaxation in graphene. (ref 6) This is a very important result because the issue of spin relaxation is among the most important in graphene spintronics due to the huge discrepancy between the long spin lifetimes expected theoretically (microseconds) and shorter lifetimes observed experimentally (hundred picoseconds). Several possible mechanisms have been proposed for the spin relaxation. This work eliminates charged impurity scattering as one of the possibilities.

II. Detailed Description of Results

(1) Spin Injection and Transport in Graphene

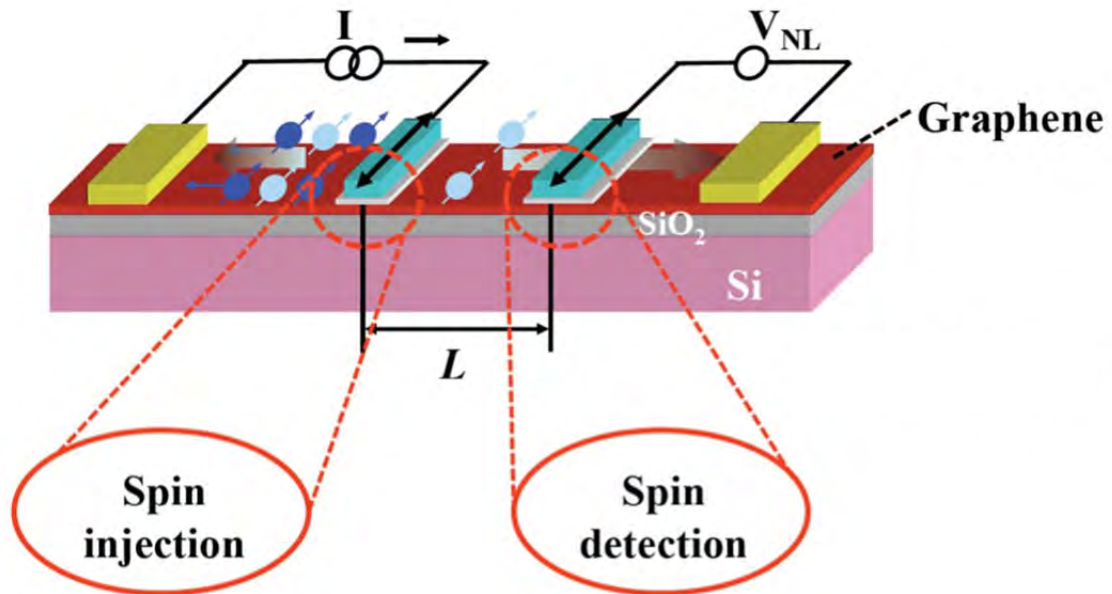


Fig. 1: Schematic drawing of a graphene spin valve in the non-local spin transport geometry.

All experiments in this section were based on nonlocal spin transport in graphene spin valves consisting of an ultrathin sheet of graphene (single or bilayer) contacted by ferromagnetic cobalt electrodes (Figure 1). The devices were connected in the non-local geometry, with a current

source to inject spins into the graphene and a voltmeter to measure the spin diffusion away from the current loop. A pure spin current (without net charge current) flows from injector to detector. The spin transport was measured in the non-local magnetoresistance geometry, where a magnetic field was applied in-plane along the long axes of the Co electrodes. Spin lifetimes were measured in the Hanle geometry, where a magnetic field was applied out-of-plane to generate spin precession of the pure spin current. The Si substrate was used as a backgate to change the carrier concentration of the graphene.

At the start of the grant period, the two overriding issues in graphene spintronics were the short spin lifetimes and the poor spin injection efficiency. One route to increasing the spin injection efficiency was to utilize a tunnel barrier to alleviate the conductance mismatch problem for spin injection. Building on our earlier results of growing atomically flat MgO on graphene via submonolayer TiO₂ seed layer, we became the first to demonstrate tunneling spin injection into graphene.

Figure 2 shows the electrical properties of graphene spin valves with Co electrodes and Co/MgO/TiO₂/graphene tunnel junctions. Figure 2a is the bias dependence of the differential contact resistance (dV/dI) of the contact. The peak near zero bias indicates the non-linearity of the I - V curve of the junction, which is characteristic of tunneling. Figure 2b shows the temperature dependence of the zero bias differential contact resistance. The slight decrease as a function of increasing temperature also indicates that the transport across the junction is via tunneling as opposed to pinholes. Together, these characteristics show that transport across the junctions is by tunneling.

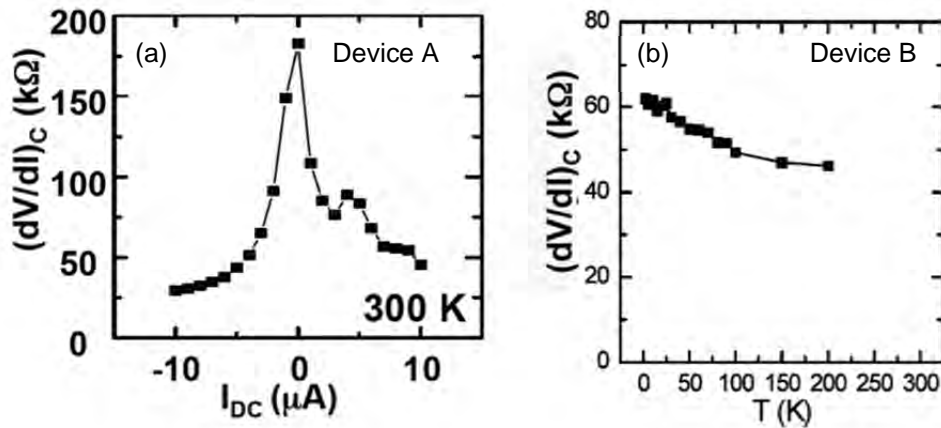


Fig. 2: Electrical characterization of contacts. (a) Bias dependence of differential contact resistance shows that the I - V curve is nonlinear. (b) Temperature dependence of zero-bias contact resistance.

Investigating the spin injection and transport in graphene spin valves with tunneling contacts proved to be very interesting [7]. Figure 3 compares the non-local spin signal for devices with transparent contacts (Figure 3a) and tunneling contacts (Figure 3b). Interestingly, for devices with similar distance between spin injection and spin detector (~ 2 microns), the non-local spin signal was 2,000 larger for the tunneling contact than the transparent contact. The spin injection efficiency, which is the spin polarization of the injected carriers, was $\sim 30\%$ for tunneling contacts while only $\sim 1\%$ for the transparent contacts. This manifested the expected enhancement

of spin injection efficiency by using tunnel barriers to alleviate the conductance mismatch problem.

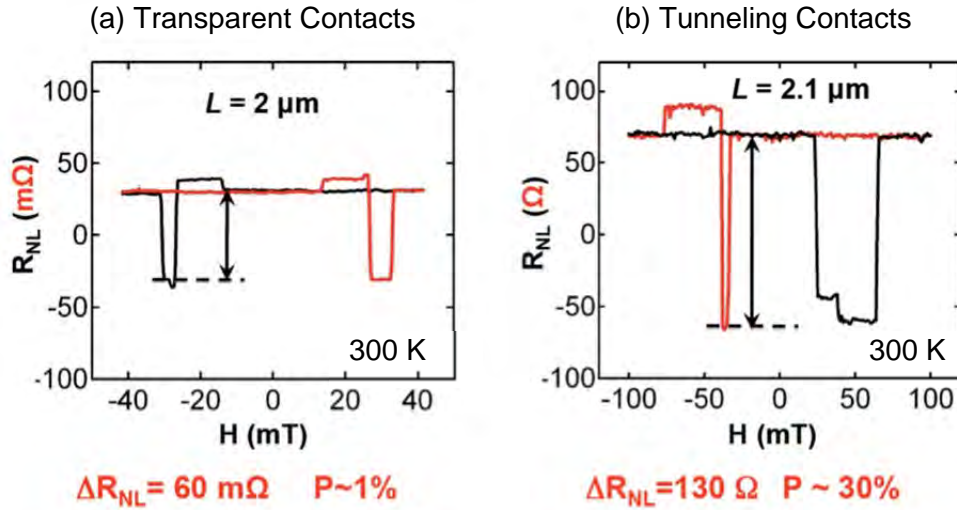


Fig. 3: Enhancement of spin injection efficiency by tunneling contacts. (a) Non-local spin transport measurement for graphene spin valve with transparent contacts. (b) Non-local spin transport measurement for graphene spin valve with transparent contacts.

Investigating the effect of tunnel barriers on spin lifetime provided a surprising result [7]. Figure 4 compares the spin lifetime measure by Hanle measurement for transparent, pinhole, and tunneling contacts. The enhancement of spin lifetime up to 771 ps revealed contact-induced effects as the origin of the strongest spin relaxation in graphene spin valves. The contact effects could be interfacial spin-flip scattering, dephasing by inhomogeneous fringe fields, or escape time effects.

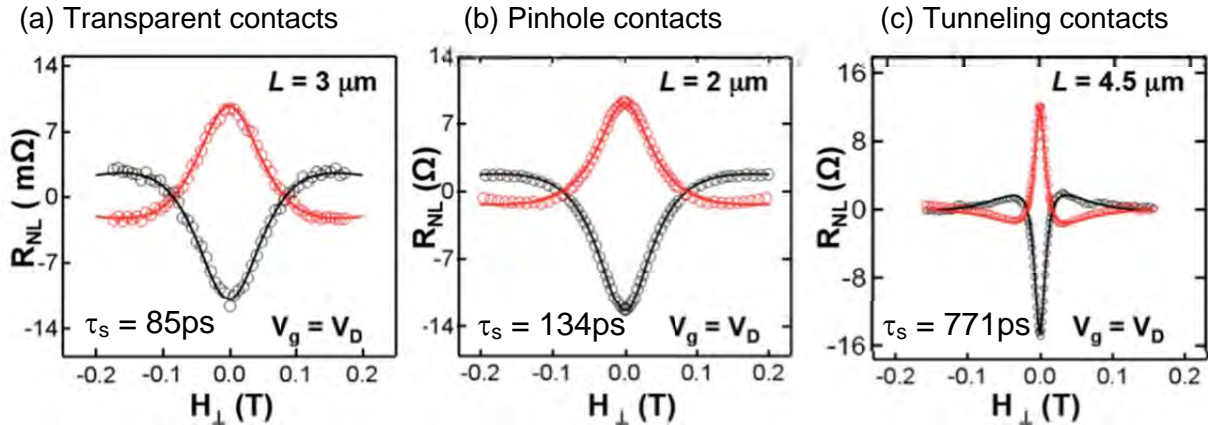


Fig. 4: Enhancement of spin lifetime due to tunneling contacts. (a-c) Hanle measurement of spin lifetime in graphene spin valve with transparent contacts (panel a), pinhole contacts (panel b), and tunneling contacts (panel c). Red (black) curve is for parallel (antiparallel) magnetization alignment of injector and detector contacts.

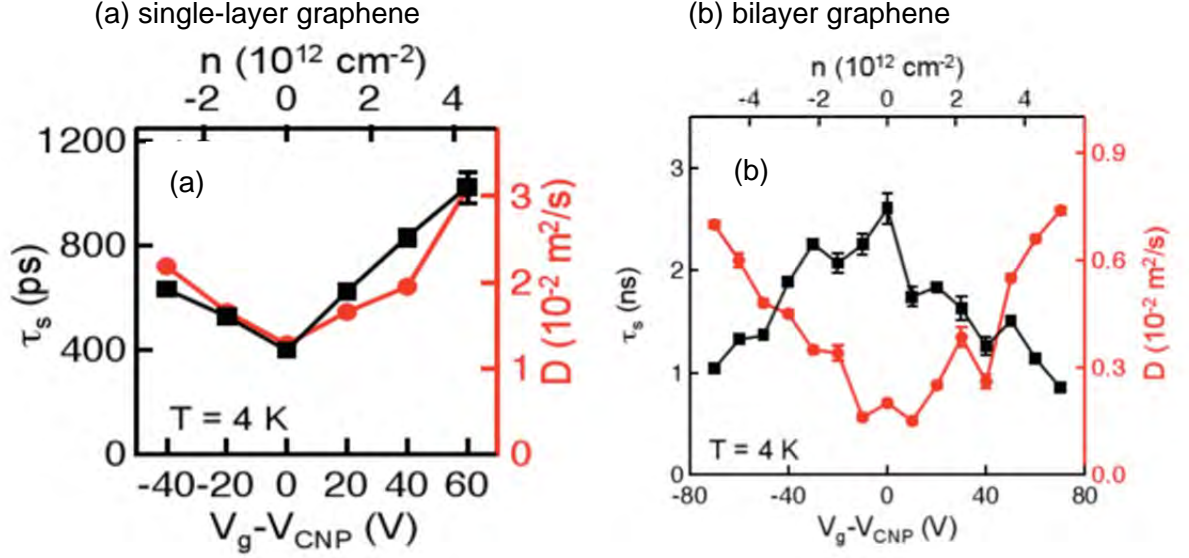


Fig. 5: Relationship between spin lifetime and diffusion coefficient in graphene. (a) As a function of gate voltage (carrier concentration), single layer graphene exhibits a similar behavior for spin lifetime and diffusion coefficient, which is characteristic of Elliot-Yafet spin relaxation. (b) As a function of gate voltage (carrier concentration), bilayer graphene exhibits opposite behavior for spin lifetime and diffusion coefficient, which is characteristic of Dyakonov-Perel spin relaxation.

Using high quality tunneling contacts, we investigated spin relaxation in single layer graphene (SLG) and bilayer graphene (BLG) [9]. At low temperatures, we found that the spin lifetimes in BLG were typically longer than SLG. The longest reported value for BLG was 6.2 ns. Also of strong interest was comparing the relationship between spin relaxation and momentum scattering (via diffusion coefficient D). In SLG, the spin lifetime τ_s and diffusion coefficient D were found to have a similar dependence on carrier concentration (Figure 5a). This suggests an Elliot-Yafet-like mechanism for spin relaxation (spin relaxation generated by momentum scattering). On the other hand, in BLG the spin lifetime τ_s and diffusion coefficient D were found to have opposite dependence on carrier concentration (Figure 5b). This suggests a Dyakonov-Perel-like mechanism for spin relaxation (spin relaxation generated by precession from internal spin-orbit fields, which is suppressed by momentum scattering). Some recent theoretical studies based on Rashba spin-orbit domains provide a possible explanation for the coexistence of Elliot-Yafet-like and Dyakonov-Perel-like properties [13].

We investigated the role of bias dependence on spin injection and spin extraction in SLG spin valves with transparent contacts [3]. The bias dependence is a topic of high interest within spintronics for semiconductor and metal systems. The unique aspect of graphene is that the polarity of the carriers can be tuned from electrons to holes. Specifically, the graphene band structure exhibits an electron-hole symmetry that does not exist in conventional semiconductors. In our experiments, we observed an asymmetry in the spin injection/extraction for electrons and holes. When the carriers were holes and the bias was for spin extraction, the non-local spin signal was reduced (Figure 6). This did not occur for spin extraction by electrons, implying a breaking of the electron-hole symmetry. We believe this broken symmetry is due to the n-type doping of graphene by the direct Co contact.

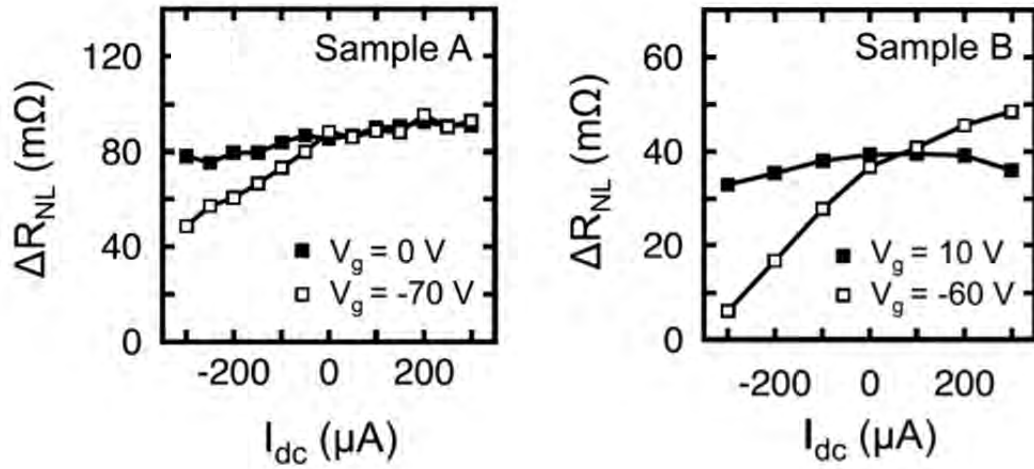


Fig. 6: Bias dependence of non-local spin signal for electrons (solid dots) and hole (open dots). For these two samples, the spin injection efficiency exhibits a sharp drop for holes under negative bias. This corresponds to hole spin “extraction”, where the holes are driven from the graphene into the Co electrode.

(2) Spin and Charge Transport in Doped Graphene

We developed an ultrahigh vacuum chamber that allows for the decoration of graphene surfaces using molecular beam epitaxy (MBE) effusion cells, *in situ* variable temperature magnetotransport measurement (15 – 300 K, 0-1000 Oersted field), and sample transfer. This enabled studies of adsorbed atoms on the surface of graphene and their effect on charge and spin transport, all without exposing the sample to air. The *in situ* approach was first used by the Fuhrer group to study the effects of potassium doping on charge transport in graphene [14].

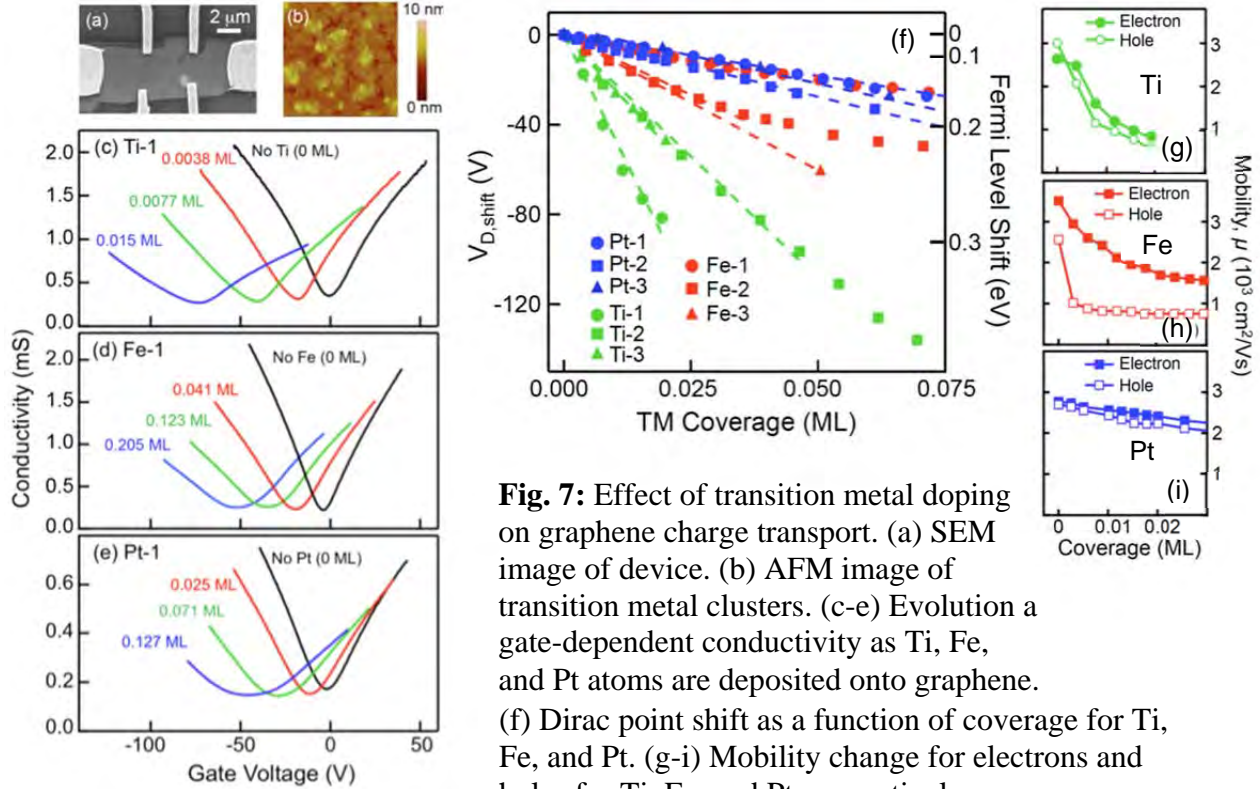


Fig. 7: Effect of transition metal doping on graphene charge transport. (a) SEM image of device. (b) AFM image of transition metal clusters. (c-e) Evolution of a gate-dependent conductivity as Ti, Fe, and Pt atoms are deposited onto graphene. (f) Dirac point shift as a function of coverage for Ti, Fe, and Pt. (g-i) Mobility change for electrons and holes for Ti, Fe, and Pt, respectively.

Our initial investigation centered on the effects of transition metal doping on charge transport in graphene [4]. To our knowledge, this was the first study of this type using transition metals. Figure 7a-7c shows the changes in gate-dependent conductivity as Ti, Fe, or Pt atoms were deposited onto the graphene surface at room temperature. In all cases, the Dirac point shifted to the left, indicating that the transition metals were donating electrons to the graphene. This was especially surprising for Pt, which has a bulk workfunction of ~6.0 eV that is much larger than graphene (~4.5 eV). In such a case, one would expect the Pt to act as an electron acceptor. This showed for atomic adsorbates or small clusters, the simple consideration of bulk workfunction cannot explain the observed behavior. The second effect was that the mobility was reduced by the transition metal dopants, as indicated by reduction of slope of the conductivity vs. gate curves. A summary of the shift in Dirac point and reduction of mobility are shown in Figures 7f-7i. Figure 7f shows results for several samples. While there were sample-to-sample variations, the main trend was that Ti produced the strongest electronic doping, while Pt produced the weakest n-type doping. This is consistent with the trend of the bulk workfunction. Figures 7g-7i show the decrease in mobility for the electrons and holes for Ti, Fe, and Pt, respectively. The Ti

exhibited the fastest reduction in mobility, which is consistent with the strongest doping (Fig. 7f) assuming charged impurity scattering. Likewise, Pt showed the slowest reduction in mobility, which is consistent with the weakest doping (Fig. 7f). Interestingly Fe showed an asymmetry of the electron and hole mobilities, which might be due to hybridization of the Fe with graphene.

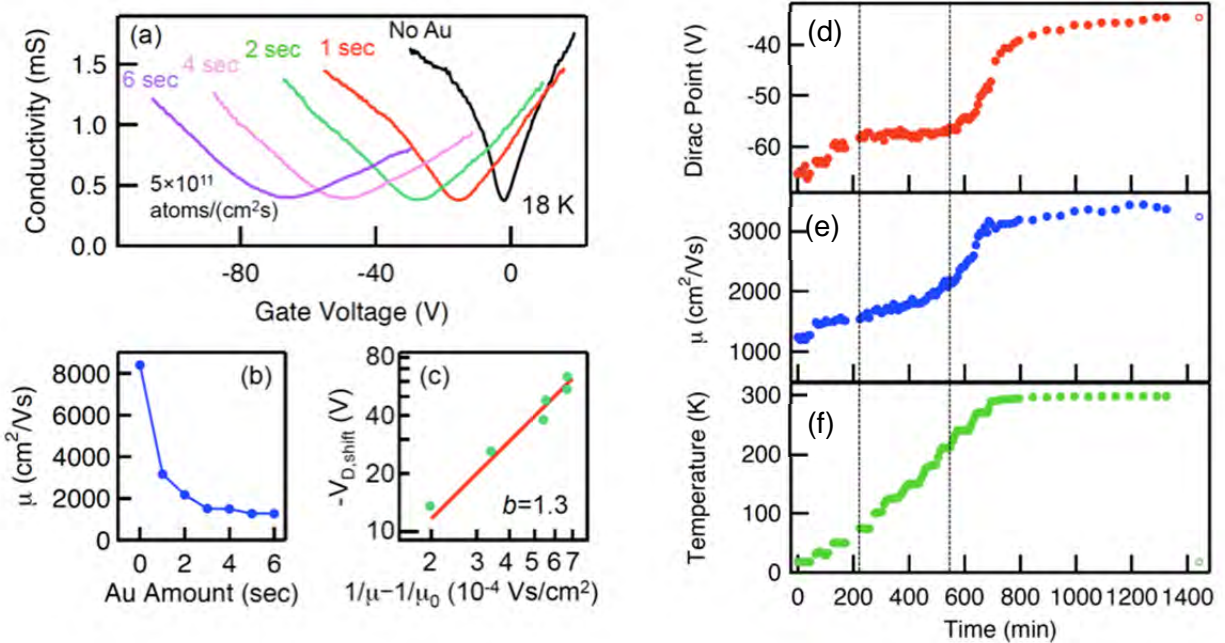


Fig. 8: Effect of cluster formation on doping and scattering by gold adatoms. (a) Gate-dependent conductivity as gold atoms are deposited onto the graphene surface at low temperature (18 K). (b) Mobility at low temperature as a function of gold coverage. (c) Relation between Dirac point shift and inverse mobility, showing a power law of 1.3 which is consistent with pointlike charged impurity scattering. (d-f) The Dirac point, mobility, and temperature, respectively, as a function of time as the sample is heated up. The final data points (open circles) are the values after a second cooldown, which shows that the changes are irreversible.

We investigated the effect of clustering of adsorbates by utilizing low temperature deposition of gold adatoms [5], which are known to have a large surface mobility at room temperature. The low temperature deposition freezes the positions of the gold atoms and subsequent annealing to room temperature allows the atoms to move and form clusters. Figure 8a shows the initial deposition at low temperature, which exhibited strong electronic doping (Dirac point shift) with nearly one electron per gold atom, similar to behavior seen for low temperature potassium doping [14]. Analyzing the relationship between Dirac point shift and inverse mobility showed a power law consistent with point-like Coulomb scatterers (Figure 8c). Figure 8d-8f shows the Dirac point shift and mobility as the sample was warmed up to room temperature. With increasing cluster size, the Dirac point shift was reduced and the mobility increased. This behavior is consistent with theoretical predictions of Katsnelson, Guinea, and Geim [15].

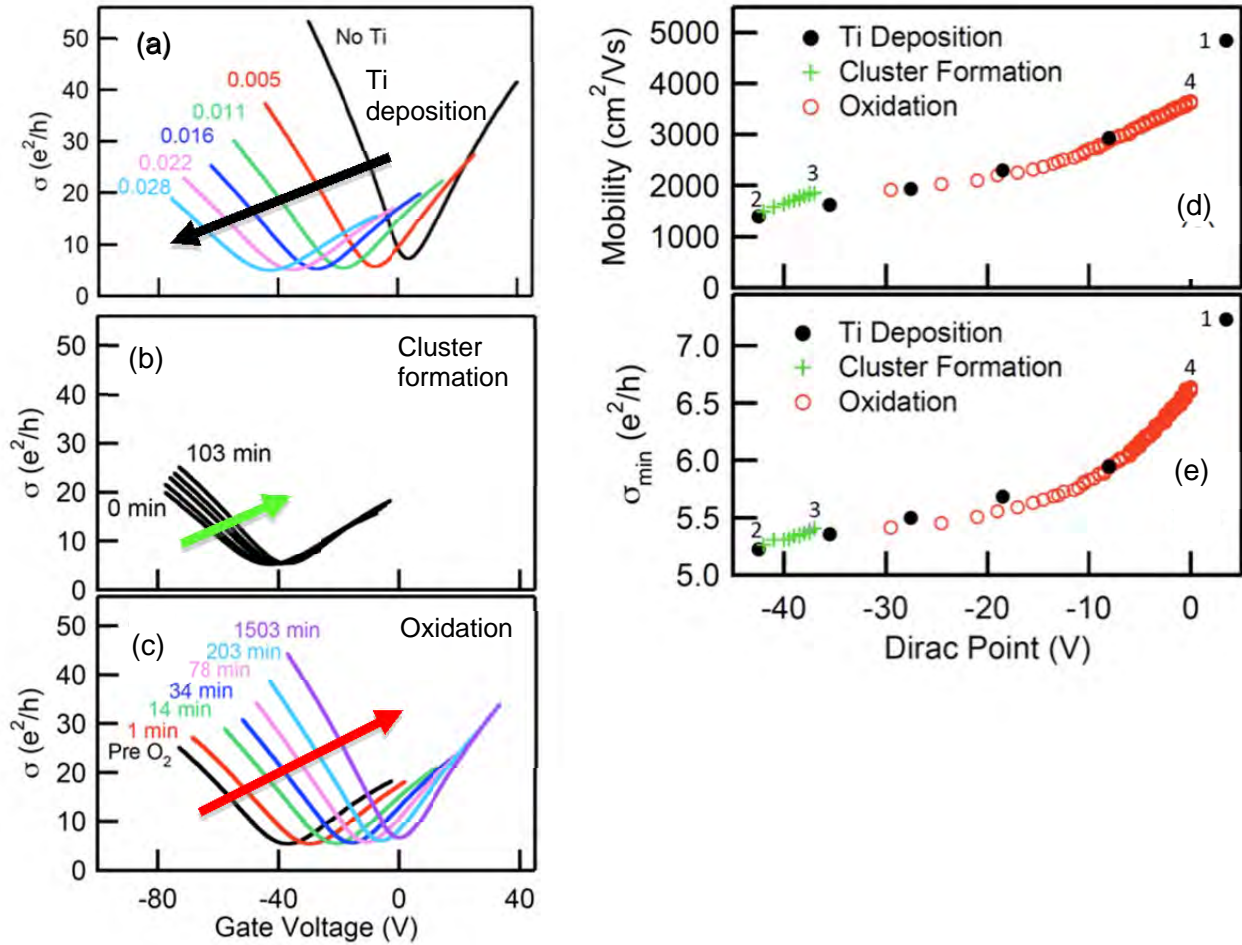


Fig. 9: Comparing metallic vs. insulating adsorbates on graphene. (a-c) Evolution of gate-dependence conductivity during metallic Ti deposition (panel a), cluster formation (panel b), and oxidation of Ti in oxygen gas to form insulating TiO₂ (panel c). (d) Evolution of mobility during this process. (e) Evolution of conductivity minimum during this process.

We also compared the effects of metallic vs. insulating adsorbates on charge transport in graphene [8]. The strategy was to deposit metallic titanium adsorbates and then post-oxidize to convert the adsorbates to insulating TiO₂. In this manner, the comparison between metallic vs. insulating was done for the same spatial distribution of adsorbates on the same piece of graphene. Figure 9 shows the gate-dependent conductivity with the initial deposition of Ti atoms (Figure 9a), cluster formation (Figure 9b), and subsequent post-oxidation (Figure 9c). The entire process was performed at room temperature. Figure 9d shows the evolution of the mobility, whereas the Figure 9e shows the evolution of the conductivity minima during this process. Both quantities are plotted against the Dirac point shift. Converting metallic Ti adsorbates to insulating TiO₂ by post-oxidation generally reversed the effect of the adsorbates. As the Ti was oxidized, the mobility increased as the Dirac point came back toward its initial value. Interestingly, the mobility extrapolated to a value lower than the initial mobility (Fig. 9d). On the other hand, the conductivity minimum extrapolated up to its initial value (Fig. 9e). Because

conductivity minima depends on the electron-hole puddles what arise from Coulomb interaction with charged impurities, while the mobility can be affected by both the charged impurity and short range scattering. The result of these extrapolations was to show that the TiO_2 adsorbates indeed contribute to short range scattering.

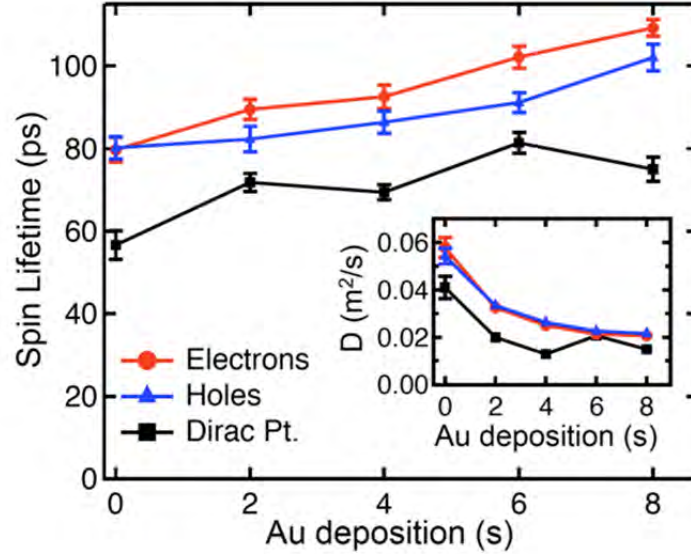


Fig. 10: Effect of Au adatom deposition on spin lifetime and diffusion coefficient (inset) for electrons (red), holes (blue), and at the Dirac point (black).

We also utilized the *in situ* approach to investigate the mechanism of spin relaxation in graphene [6], one of the major topics in graphene spintronics. To investigate the role of charged impurity scattering on spin relaxation, we utilized gold adsorbates deposited at low temperature. From earlier studies (Figure 8), low temperature gold was found to act as point-like charged impurity scatterers. In addition, the gold-graphene chemical interaction was expected to be weak. The fact that gold could introduce additional spin-orbit coupling was not ideal, but gold remained as the best choice for charge impurity scattering of all materials that we had examined up to that point. Figure 10 shows the main result, which was that the addition of charged impurity scattering from gold did not reduce the spin lifetime, even though substantially reduced the mobility. In fact, the spin lifetime exhibited a slight increase. The lack of a major decrease in spin lifetime proved that spins are robust against charged impurity scattering [6].

Papers citing this grant:

1. W. Han, K. Pi, W. Bao, K. M. McCreary, Y. Li, W. H. Wang, C. N. Lau, and R. K. Kawakami, *Electrical detection of spin precession in single layer graphene spin valves with transparent contacts* Appl. Phys. Lett. **94**, 222109 (2009).
2. W. Han, K. Pi, W. H. Wang, K. M. McCreary, Y. Li, W. Bao, P. Wei, J. Shi, C. N. Lau, and R. K. Kawakami, *Spin transport in graphite and graphene spin valves* Proc. SPIE **7398**, 7398819 (2009).
3. W. Han, W. H. Wang, K. Pi, K. M. McCreary, W. Bao, Y. Li, F. Miao, C. N. Lau, and R. K. Kawakami, *Electron-hole asymmetry of spin injection and transport in single-layer graphene* Phys. Rev. Lett. **102**, 137205 (2009).
4. K. Pi, K. M. McCreary, W. Bao, W. Han, Y. F. Chiang, Y. Li, S.-W. Tsai, C. N. Lau, and R. K. Kawakami, *Electronic doping and scattering by transition metals on graphene* Phys. Rev. B **80**, 075406 (2009).
5. K. M. McCreary, K. Pi, A. G. Swartz, W. Han, W. Bao, C. N. Lau, F. Guinea, M. I. Katsnelson, and R. K. Kawakami, *Effect of cluster formation on graphene mobility* Phys. Rev. B **81**, 115453 (2010).
6. K. Pi, W. Han, K. M. McCreary, A. G. Swartz, Y. Li, and R. K. Kawakami, *Manipulation of Spin Transport in Graphene by Surface Chemical Doping* Phys. Rev. Lett. **104**, 187201 (2010).
7. W. Han, K. Pi, K. M. McCreary, Y. Li, J. J. I. Wong, A. G. Swartz, and R. K. Kawakami, *Tunneling Spin Injection into Single Layer Graphene* Phys. Rev. Lett. **105**, 167202 (2010).
8. K. M. McCreary, K. Pi, and R. K. Kawakami, *Metallic and insulating adsorbates on graphene*, Appl. Phys. Lett. **98**, 192101 (2011).
9. Wei Han, R. K. Kawakami, *Spin Relaxation in Single-Layer and Bilayer Graphene*, Phys. Rev. Lett. **107**, 047207 (2011).
10. Wei Han, J. R. Chen, K. M. McCreary, Hua Wen, and R. K. Kawakami, *Enhanced spin injection efficiency and extended spin lifetimes in graphene spin valves*, Proc. SPIE, **Vol. 8100**, 81000Q (2011)
11. Wei Han, K.M. McCreary, K. Pi, W.H. Wang, Yan Li, H. Wen, J.R. Chen and R.K. Kawakami, *Spin transport and relaxation in graphene*, J. Magn. Magn. Mater. **324**, 369-381 (2012) (Review paper, online in 2011).

Additional references:

12. N. Tombros, C. Jozsa, M. Popinciuc, H. T. Jonkman, and B. J. Van Wees, *Electronic spin transport and spin precession in single graphene layers at room temperature*, Nature **448**, 571 (2007).
13. H. Tong, and M. W. Wu, *Electron spin diffusion and transport in graphene*, Phys. Rev. B **84**, 045304 (2011).
14. J. H. Chen, C. Jang, S. Adam, M. S. Fuhrer, E. D. Williams, and M. Ishigami, *Charged-Impurity Scattering in Graphene*, Nature Physics **4**, 377 (2008).
15. M. I. Katsnelson, F. Guinea, and A. K. Geim, *Scattering of Electrons in Graphene by Clusters of Impurities*, Phys. Rev. B **79**, 195426 (2009).